

## Investigation of the mechanical properties on hybrid deposition and micro-rolling of bainite steel

Youheng Fu\*, Haiou Zhang\*, Guilan Wang†, Huafeng Wang†

\*State Key Laboratory of Digital Manufacturing Equipment and Technology,  
Huazhong University of Science and Technology, Wuhan 430074, PR China

†State Key Laboratory of Materials Processing and Die & Mould Technology,  
Huazhong University of Science and Technology, Wuhan 430074, PR China

### Abstract

Wire and arc additive manufacturing (WAAM) is a novel technology with high efficiency and low cost for mass popularity. Whereas, the lack of deposition accuracy and microstructure performances are still restricting its ongoing development. In this paper, hybrid deposition and micro-rolling (HDMR) process has been used to eliminate the anisotropy in WAAM bainitic steel samples. For the problems of deficient deformation and larger remelting area due to deeper penetration and higher temperature gradient, an initially optimized micro-rolling morphology has been proposed. The results show: the tensile strengths of finished part are 1275MPa, 1256MPa, 1309MPa for transverse (X), longitudinal (Y), perpendicular (Z) directions respectively. The elongation of three directions are 17.4%, 16.6%, 17.7% respectively. The impact toughness is 99J/cm<sup>2</sup> and the average grain size reaches about 7 $\mu$ m. Compared to the traditionally heavy rolling equipment, micro roller this paper used has transformative cost advantage to achieve high values of comprehensive mechanical properties.

**Keywords:** additive manufacturing; bainite steel; mechanical properties; micro rolling; welding

### 1 Introduction

Bainite steel is a type of structural material which has been widely used in many major industries of the national economy such as railway, oil pipeline, engineering machinery, bridge, vehicle, architecture and aerospace areas, where high strength, high ductility and good solderability are required to adapt to variously complex conditions of service owing to the low cost, perfect weldability and excellent comprehensive mechanical properties[1]. There is no doubt that bainite steel represents the development direction of modern high-performance steel.

The additive manufacturing (AM) is a technique based on the dispersion-deposition principle, which takes layer by layer overlapping manner to have a “bottom-up” freeform fabrication from CAD model data. AM has the potential to reduce material

cost and lead-time due to the capability of near-net successive shape fabrication, is nowadays among the most studied processes[2,3]. Powder bed, blown powder and wire feed are the main AM feeding techniques, while the most common heat sources are laser, electron beam or electric arc.

The Wire and Arc Additive Manufacturing (WAAM) is one of AM that using electric arc as heat source and combining wire as feedstock, has been initially—investigated for large scale metallic components deposition by using submerged arc welding (SAW) since 1970[4]. There are a number of welding processes such as Gas Metal Arc Welding (GMAW), Gas Tungsten Arc Welding (GTAW) and Plasma Arc Welding (PAW) have been used for WAAM. High energy efficiency and deposition rates, low material and equipment costs, and good structure integrity make WAAM to develop rapidly, especially in the deposition of large thick-walled parts with low and medium complexity morphology[5]. Among other two useful AM techniques, Selected Laser Melting (SLM) is sensitive to a part of metal such as aluminum alloy and copper alloy; Electron Beam Melting (EBM) part size is determined by equipment forming cylinder and vacuum chamber, and both of them have high manufacturing accuracy and cost compared with WAAM. Moreover, the lack of fusion, cracking, porosity, residual stresses and distortion are the most important issues that slow all of the AM wider application. Fortunately, these bottleneck problems have been overcome gradually by using a series of actively thermodynamic controlling methods and subsidiary processes such as milling, peening, electromagnetic stirring and post heat treatment[6-9].

Due to the procedure of rapid heating and cooling result in columnar grains growth, anisotropic properties have been found in all kinds of additive manufacturing parts made by high energy beam including laser, electron beam and arc. This situation can seriously affect the reliability on performance and quality of significant components with complex conditions. As we all known, the fine equiaxed grains have excellent mechanical properties which can hinder the expanding of cracks efficiently on account of the number of grain boundaries increased. Recent studies by Dinda et al.[10] used direct metal deposition technology to fabricate Inconel 625 samples, which found the full recrystallized equiaxed structure can be obtained when the as-deposited sample was annealed at 1200°C for 1h followed by cooling in air. However, the grain size distribution is inhomogeneous which ranks from 100~250µm.

Rolling was found to result in a dramatic method for transforming the dendritic structures into equiaxed grains due to the deformation induced recrystallization[11]. Therefore, many domestic and foreign scholars have done a lot of researches for WAAM with rolling successively. Williams et al.[12-16] proposed to use high-pressure interpass rolling for reducing residual stress and distortion on account of the plastic deformation over the entire weld cross-section, and for high rolling loads tensile weld stresses have even turned into compressive ones. Finally, microstructure refinement converts the deposited anisotropic properties into isotropic ones. However, the “profiled” and “slotted” roller they have used cannot implement on non-linear deposits especially the intersecting features. Moreover, the separated casting and rolling process has higher requirement of equipment tonnage, greater

tendency toward cracks and inhomogeneous grain size distribution due to the lower rolling temperature especially for the metal parts with poor toughness.

Previously, hybrid deposition and micro-rolling (HDMR) was successfully tried on directly fabricating large thin-wall metal component with high quality, low cost and great efficiency, which realized the integration of casting and rolling[17]. Compared with high-pressure interpass rolling process, the HDMR can obtain finer equiaxed grains by using smaller device. However, the mechanisms of grain refinement have not been discussed deeply. Furthermore, the HDMR only applied for manufacturing wall component before.

In this paper, HDMR process has been used to eliminate the anisotropy of bainitic steel WAAM part with multi-layer and multi-pass welding, and the optimization for refined crystalline strengthening mechanism has also been discussed in depth.

## **2 Experimental works**

### **2.1 Material and procedure**

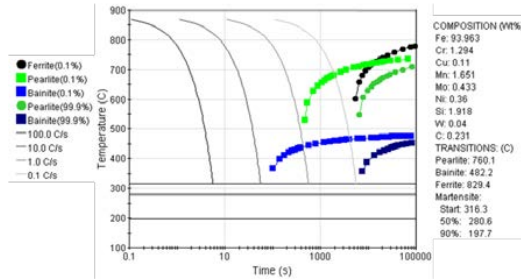
A commercially bainite steel was chosen for this study, which was used in form of wire and substrate in the WAAM and HDMR samples. The chemical composition of bainite steel is shown in Table 1. Fig. 1 shows the continuous cooling transformation (CCT) curve of bainite steel, which was simulated by using JmatPro software.

Fig. 2 shows the schematic diagram of HDMR process (the X, Y and Z directions are defined in this figure). The HDMR process was performed on a custom-made flat rolling rig, equipped with a SAF•FRO DIGI@WAVE™ 280 metal inert gas (MIG) welding machine supply. Moreover, a three-axis computer numerical control (CNC) machine acted as motion platform and the industrial personal computer (IPC) was used to process the signals. The roller followed with the torch to move and begun to roll on the sample surface according to the prescribed trajectory when received the arc striking signal. Therefore, metal samples were fabricated by hot rolling immediately after deposition because of the shorter distance from torch to roller. The loads were applied with a low power motor and the force was monitored with a pressure sensor placed between the screw rod and the roller rack. It must be pointed out that the rolling rig this study has proposed can only work for hot rolling due to the micro organization, and the max output pressure is 12KN.

In order to look into the different microstructure and property reflections between WAAM and HDMR comprehensively, three kinds of experimental samples with approximately 80mm long have been prepared, were single-pass single-layer, single-pass multi-layer and multi-pass multi-layer respectively. Both samples were produced in similar welding process and were deposited on similar rolled structural substrates with dimensions 100mm×40mm×10mm. Prior to deposition the substrate surfaces were preheated to 250℃ and ground to remove oxide scale and rust. Furthermore, the sample was allowed to cool below 250℃ but not less than 200℃ before each new layer was deposited. To realize the quick and stable clamp, the flat tong has been used. The original welding conditions for WAAM and HDMR have been presented in Table 2.

**Table 1 Chemical composition of substrate metal and filler wire used (wt.%)**

| C   | Si  | Mn  | S   | Mg  | Cr  | Ni  | Mo  |
|-----|-----|-----|-----|-----|-----|-----|-----|
| 0.2 | 1.9 | 1.6 | 0.0 | 0.0 | 1.2 | 0.3 | 0.4 |
| 310 | 180 | 510 | 120 | 005 | 940 | 600 | 330 |
| Cu  | Ti  | V   | Nb  | W   | Co  | Zr  | B   |
| 0.1 | 0.0 | 0.0 | 0.0 | 0.0 | 0.0 | 0.0 | 0.0 |
| 100 | 890 | 100 | 030 | 400 | 220 | 010 | 004 |



**Fig. 1 The simulated CCT curve of bainite steel**

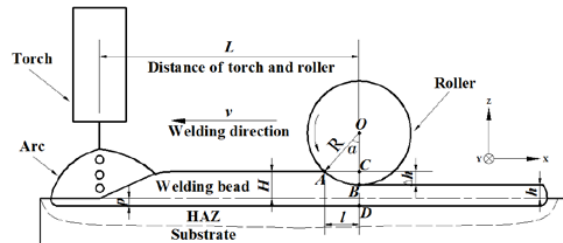


**Fig. 2 Schematic diagram of HD MR process**

**Table 2 Original welding conditions**

| Polarity                        | DCRP                      |
|---------------------------------|---------------------------|
| Mode of operation               | Constant current mode     |
| Wire diameter (mm)              | 1.2                       |
| Wire feed speed (m/min)         | 5.0                       |
| Current (A)                     | 194                       |
| Arc voltage (V)                 | 27.6                      |
| Welding speed (mm/min)          | 600                       |
| Shielding gas                   | 95% Ar+5% CO <sub>2</sub> |
| Shielding gas flow rate (L/min) | 17                        |
| Nozzle to plate distance (mm)   | 12                        |
| Welding width (mm)              | 9.8                       |
| Welding reinforcement (mm)      | 1.8                       |
| Welding penetration (mm)        | 1                         |

## 2.2 Thermo-simulation compression experiment

On account of obtaining optimum HD MR process, the thermo simulation compression experiment has been proposed, which was carried out on Gleeble-3500

thermo-simulation machine by using  $\phi 10\text{mm}\times 15\text{mm}$  cylindrical specimens. The specimens were first heated to  $1100^{\circ}\text{C}$  at  $10^{\circ}\text{C}/\text{s}$  and held for 5min to eliminate thermal gradients, then cooled at  $5^{\circ}\text{C}/\text{s}$  to the deformation temperatures ( $600^{\circ}\text{C}$ ,  $750^{\circ}\text{C}$  and  $900^{\circ}\text{C}$ ) and held for 15s to uniform temperature distribution before hot compression with a specified deformation rate ( $0.1\text{s}^{-1}$ ,  $1\text{s}^{-1}$  and  $5\text{s}^{-1}$ ) and degree (60% of the height). Subsequently, the deformed specimens were cooled in the air due to simulate the cooling process of welding as shown in Fig. 3. All of the experiments were set in argon shielding. Furthermore, the specimens after deformation were sectioned along the longitudinal compression axis by using wire-cut and then were inlaid into phenolic resin, which were also shown in Fig. 3. Finally, the optical microstructures of inlaid specimens were prepared by using ground, polished and etched with 4% nital.

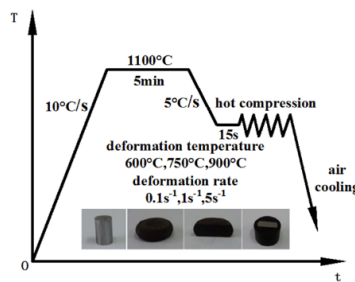


**Fig. 3 Process flow diagram of thermo simulation compression experiment**

### 3 Results and Discussions

#### 3.1 Rolling parameters of HDMMR

The true stress-strain curves at different temperatures and strain rates are shown in Fig. 4. As we all know, the true stress decreases with the increase of deformation temperature and decrease of deformation rate due to the higher kinetic energy of atoms and longer time for energy accumulation[18]. However, the abnormal tendency was occurred at  $600^{\circ}\text{C}$ , which can be seen that the true stress decreases with the increase of deformation rate. The reason could be that the deformation temperature at  $600^{\circ}\text{C}$  is too lower and the temperature effect became more sensitive with the increasing deformation rate.

Fig. 5 shows the microstructures of deformed specimens under different conditions. As shown in Fig. 5(a), some coarse grains were obtained from the effects of strain induced grain boundary migration, and most of the microstructures show fully deformation structure. A mixture of recrystallized and deformed microstructures can be seen in Fig. 5(b). Moreover, the obvious deformation textures enhance the direction of intensity which will reduce the impact toughness. When the deformation temperature increases to  $900^{\circ}\text{C}$ , the microstructure has no deformed characteristic. It can be seen from Fig. 5(c) and Fig. 5(d) that fully and homogeneously equiaxed grain structures were developed in the bainite steel deformation at the temperature of austenite non-recrystallization region. Therefore,  $900^{\circ}\text{C}$  was set as the original deformation temperature of HDMMR by controlling the distance of torch and roller.

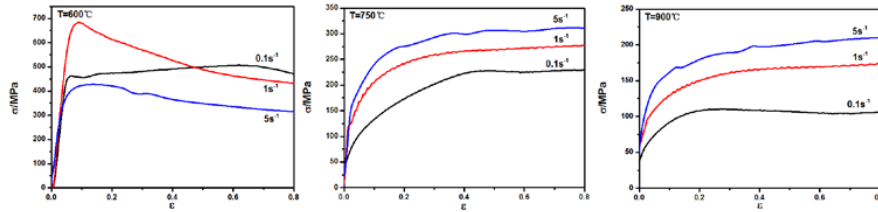


**Fig. 4 True stress-strain curve for bainite steel under different conditions**

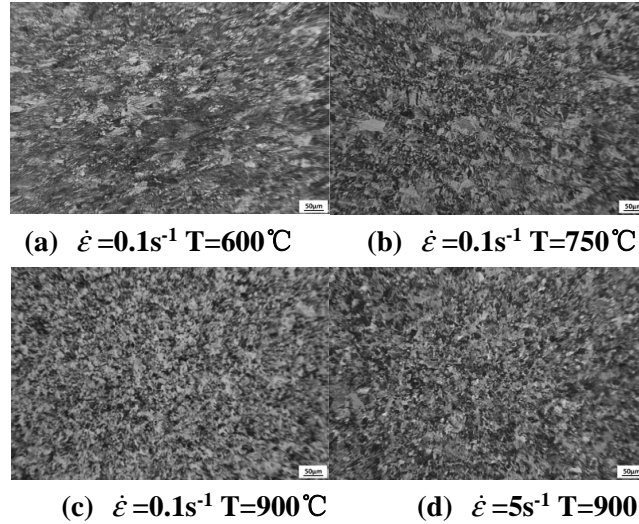


**Fig. 5 Microstructure for bainite steel under different conditions**

The controlling of constant roll gap and constant roll pressure were two methods for steel rolling. However, the WAAM is an unsteady process with repeated rapid heating and cooling thermal cycling which results in uneven heat distribution. With the increase of samples height, there will be always an error between the actual and theoretical dimensions. It should be noted that the micro roller this study has used is sensitive to the mutations of welding reinforcement, and 1mm deviation may lead to the substantial increase of rolling pressure (more than 5000N). It is difficult to obtain a completely smooth weld to realize the controlling of constant roll gap. Therefore, the controlling of constant roll pressure is chosen to be used in HDMM. Fig. 6 shows the force-stroke curve of deformed specimens under different conditions. It can be seen that the maximum force is from 2000N to 4000N when the specimens were deformed at 900°C with different deformation rates. However, compared with the theory experiment under ideal conditions, the HDMM has its unique feature that the presence of temperature gradient along transverse section makes greater rolling pressure. Hence, 5000N was set as the original deformation pressure of HDMM to obtain good rolling effects. It is obvious that the rolling parameters exist deviations between actual and theoretical values due to the uneven temperature distribution during HDMM process.

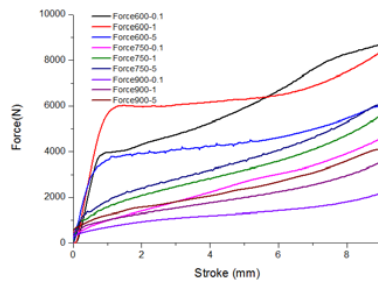


**Fig. 6 Force-stroke curve for bainite steel under different conditions**

### 3.2 HDMR experimental results and discussions

#### 3.2.1 Macrostructure and microstructure

The optical macrostructures of the transverse section of the single-pass single-layer samples produced with WAAM and HDMR are shown in Fig. 7. From Fig. 7(a), it can be seen that the sample of WAAM has an initially optimized micro-rolling morphology with shallower penetration and larger ratio of width to reinforcement by using the welding process shown in Table 2. To obtain the conditions specified in rolling temperature and pressure (900°C and 5000N), the thermal infrared imager and pressure sensor have been used to acquire data in real time. Fig. 7(b) shows the macrostructure of single-pass single-layer sample after rolling that using the initially optimized WAAM morphology of Fig. 7(a), which has a uniform deformation and flat surface. In contrast, Fig. 7(c) shows that the non-optimized HDMR sample using pulse mode has a fingerlike penetration, and it is difficult to make a deformation in this zone. Moreover, the larger remelted areas lead to a sharp weakening of the strengthening effects of deformation.



**Fig. 7 Optical macrostructure of (a) optimized WAAM, (b) optimized HDMR and (c) non-optimized HDMR single-pass single-layer**

To study the refined crystalline strengthening effects of HDMR process on microstructures and mechanical properties, the single-pass multi-layer and multi-pass multi-layer samples were produced with the same deposition parameters. The optical graphs of the transverse section of the single-pass multi-layer samples are shown in Fig. 8. Both samples were etched in a hot solution of saturated picric acid. For WAAM sample, the microstructure mostly consists of columnar dendrites, which grew epitaxially from the partially remelted grains of previous layer. The growth directions of the columnar dendrites are opposite to the resultant heat flux direction. In addition, the grain morphologies of each layer are composed of three regions because of the progressive decrease and then increase of the cooling rate from the

bottom to the top part of the melt pool. However, due to the partial remelting of the upper part of the previous layer, there are only two regions can be seen at each layer except for the topmost layer. The bottom part of each layer shows typical fine dendritic structure and the top shows columnar structure. On the other hand, the dimensions of columnar dendrites increase gradually with the sample produced layer by layer results in the declining heat dissipation. For HDMR sample, Fig. 8(d) shows that fully equiaxed grain structure was developed successfully due to the recrystallized procedure. The average deformation rate is  $0.8s^{-1}$  and the average rolling deformation is 44.4%. It must be pointed out that the grain refinement level in this micro rolling process is far better than in traditional forging. Firstly, the initial welding morphology with shallower penetration and larger ratio of width to reinforcement has provided a solid foundation for the quality and homogeneity of deformation. Secondly, the deformation at the temperature of austenite non-recrystallization region introduce large scale deformation band which can increase the nucleation rate greatly, and the larger radiation area make the samples cool immediately after deformation. It is easily to store distortion energy and prevent grain growth. Thirdly, the larger HAZ region can increase the deformation of previously deposited layers due to the decrease of temperature gradient. Finally, the smaller remelted area lead to the preservation of structure continuity. Moreover, the fully equiaxed grains derived from the special static recrystallization have very fine diameter about  $7\mu m$  due to the fast cooling rate and the grain size distribution is homogeneous. According to the GBT6394-2002, the average grain sizes of HDMR sample can be decided to grade 11~12 which is achieving the level of ultra-fine grain.

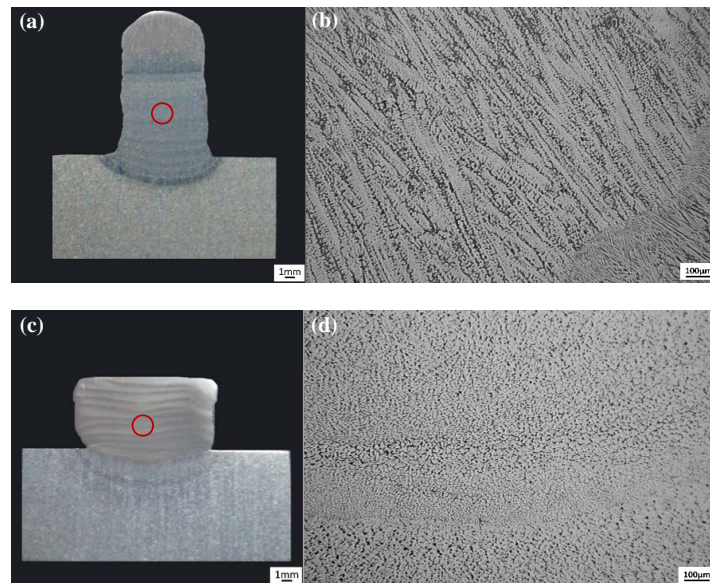


**Fig. 8 Optical (a) WAAM macrostructure, (b) WAAM microstructure, (c) HDMR macrostructure and (d) HDMR microstructure of single-pass multi-layer**

As described previously, the welding and rolling parameters this study has used can obtain a smooth surface with narrowly arch boundary as shown in Fig. 7(b). Therefore, compared with the traditional WAAM process, a tiny overlapping ratio (23.5%) has

been used to produce the dense samples with no relevant defects such as cracks, pores and lack of fusion in this paper as shown in Fig. 9(a). It should be noted that the tiny overlapping ratio not only can reduce the possibility of defects, but also can decrease the deformation resistance from previously adjacent pass. Hence, the HDMR process provides a novel way for the full transformation of columnar dendrites to equiaxed grains during the production of multi-pass multi-layer samples, which can be seen in Fig. 9(b). It should be also pointed out that the hot deformation can weaken the degree of crater collapse without arc stopping control and reduce the residual stress.

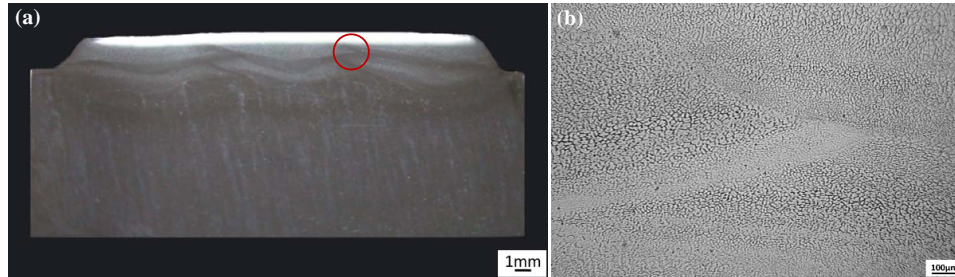


**Fig. 9 Optical (a) macrostructure and (b) microstructure of multi-pass multi-layer**

### 3.2.2 Mechanical properties

In order to assess the mechanical properties such as strength, plasticity and toughness of WAAM and HDMR samples, the tensile and impact toughness tests have been conducted. The tensile specimens had a rectangle shape with a gauge length of 10mm and a  $2.2 \times 1.2$ mm cross section as shown in Fig. 10, which were tested on the AG-100KN electronic universal testing machine with 0.5mm/min stretching rate at room temperature. The tensile test results are presented in Table 3. It can be seen that the average tensile strength and elongation of WAAM samples are 1258MPa/11.0pct, 1019MPa/4.6pct, 1286MPa/10.9pct for transverse (X), longitudinal (Y), perpendicular (Z) directions respectively, which exhibited a strong anisotropy due to the growth direction of columnar grains and the poor microstructures in fusion zone. As we all known, the growth directions of columnar grains are mostly perpendicular to the substrate and vary at different location of each layer depending upon the local cooling rate and heat flux direction. In addition, the fusion zones of adjacent pass and layer always have some harmful structures which can reduce the mechanical performances of samples. Therefore, the longitudinal samples of WAAM show poor mechanical properties which are due to be pointing roughly toward the transverse to the direction of columnar grain growth and containing some fusion zones. In comparison, the HDMR samples tested from the X, Y and Z deposited directions shown an apparent isotropy with the average tensile strength and elongation are 1275MPa/17.4pct, 1256MPa/16.6pct, 1309MPa/17.7pct because of the fully refined crystalline strengthening, and the reason for the nuances of mechanical properties are simply that the grain size distribution near the overlapping zone is uneven attributed to the uneven deformation and cooling as shown in Fig. 9(b). It

should be noted that the average tensile strength and elongation of traditionally forged bainite steel are 1240MPa/10.0pct. Moreover, the average impact toughness of HDMR samples is 99J/cm<sup>2</sup>, which is three times over WAAM. The scanning electron microscope (SEM) morphology of tensile fracture surface also illustrated that the plasticity of HDMR sample is significantly higher than WAAM as shown in Fig. 11. Because of the time limit, the fatigue performance test has not been studied in this paper.

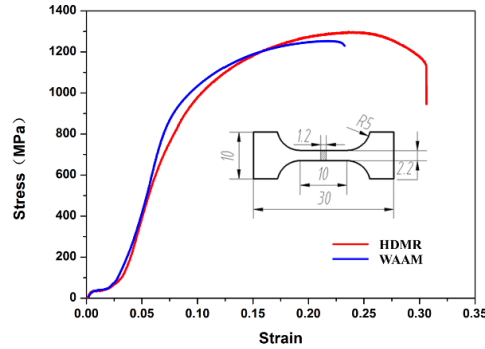
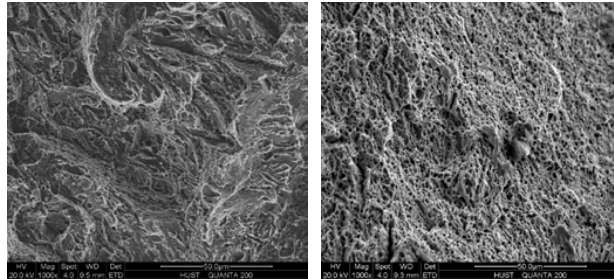


**Fig. 10 Tensile strength comparison of HDMR and WAAM**  
**Table 3 Comprehensively mechanical properties comparisons of HDMR and WAAM**

|      | Tensile strength(MPa) |      |      | Elongation(%) |      |      |
|------|-----------------------|------|------|---------------|------|------|
|      | X                     | Y    | Z    | X             | Y    | Z    |
| HDMR | 1275                  | 1256 | 1309 | 17.4          | 16.6 | 17.7 |
| WAAM | 1258                  | 1019 | 1286 | 11.0          | 4.6  | 10.9 |



**(a)WAAM**

**(b)HDMR**

**Fig. 11 The SEM morphology of tensile fracture surface**

#### 4 Conclusions

HDMR has been investigated as a method for eliminating the anisotropy, and further achieving overall refined crystalline strengthening in the WAAM bainitic steel samples. The main conclusions drawn from this comparative microstructures and mechanical properties on the WAAM and HDMR samples are listed below:

1. The optimum HDMR process shows good reactions with the deformation temperature of 900 °C, deformation force of 5000 N, average rolling deformation of 44.4%, and average deformation rate of 0.8 s<sup>-1</sup>.

2. The initially optimized micro-rolling morphology with a shallow penetration and a large ratio of width to reinforcement can obtain a uniform deformation and a flat surface for the HDMR sample.
3. In transverse cross section, the microstructure of the WAAM sample contains a lot of columnar dendrites, while having fully equiaxed grain structure in the HDMR sample.
4. The average tensile strength/elongation of the WAAM samples are 1258 MPa/11.0 pct, 1019 MPa/4.6 pct, 1286 MPa/10.9 pct for the transverse (X), longitudinal (Y), perpendicular (Z) directions, respectively, while the corresponding values for HDMR samples are 1275 MPa/17.4 pct, 1256 MPa/16.6 pct, 1309 MPa/17.7 pct. In addition, the average impact toughness of HDMR samples is 99 J/cm<sup>2</sup>, which is three times larger than that of the WAAM samples.
5. The average grain size of the bainite steel HDMR built samples is about 7 μm, and the anisotropy in WAAM samples has been eliminated.

### Acknowledge

This work was supported by the National Science Foundation of China (E050902, E041604). The authors wish to thank Li P, Wang X, Zhou XM, Wang XP, Chen QY and Wang R for their support to carry out experimentation works.

### References

- [1]Yang JR, Huang CY, Wang SC. The development of ultra-low-carbon bainitic steels[J]. *Mater & Design*, 1992, 13(6):335-338
- [2]Frazier W E. Metal Additive Manufacturing: A Review[J]. *Journal of Materials Engineering & Performance*, 2014, 23(6):1917-1928.
- [3]Szost B A, Terzi S, Martina F, et al. A comparative study of additive manufacturing techniques: Residual stress and microstructural analysis of CLAD and WAAM printed Ti–6Al–4V components[J]. *Materials & Design*, 2015, 89:559-567.
- [4]Kazanas P, Deherkar P, Almeida P, et al. Fabrication of geometrical features using wire and arc additive manufacture[J]. *Journal of Engineering Manufacture*, 2012, 226(6):1042-1051.
- [5]Williams S W, Martina F, Addison A C, et al. Wire + Arc Additive Manufacturing[J]. *Materials Science & Technology*, 2015, 00(0):1-7.
- [6]Withers P J. Residual stress and its role in failure[J]. *Reports on Progress in Physics*, 2007, 70(12):2211-2264.
- [7]Song Y-A, Park S. Experimental investigations into rapid prototyping of composites by novel hybrid deposition process [J]. *Journal of Materials Processing Technology*, 2006, 171(1): 35-40.
- [8]Zhou XM, Zhang HO, Wang GL, et al. Numerical simulation and experimental investigation of arc based additive manufacturing assisted with external longitudinal static magnetic field. *Proceedings of 26th International Solid Freeform Fabrication Symposium*, 2015,p156.

- [9] Bai X, Zhang H, Wang G. Modeling of the moving induction heating used as secondary heat source in weld-based additive manufacturing[J]. *International Journal of Advanced Manufacturing Technology*, 2015, 77(1-4):717-727.
- [10] Dinda G P, Dasgupta A K, Mazumder J. Laser aided direct metal deposition of Inconel 625 superalloy: Microstructural evolution and thermal stability[J]. *Materials Science & Engineering A*, 2009, 509(1-2):98-104.
- [11] Li F, Shi W, Bian N, et al. Effect of Accumulative Strain on Grain Refinement and Strengthening of ZM6 Magnesium Alloy During Continuous Variable Cross-Section Direct Extrusion[J]. *Acta Metallurgica Sinica*, 2015, 28(5):649-655.
- [12] Colegrove P A, Martina F, Roy M J, et al. High Pressure Interpass Rolling of Wire + Arc Additively Manufactured Titanium Components[J]. *Advanced Materials Research*, 2014, 996:694-700.
- [13] Colegrove P A, Coules H E, Fairman J, et al. Microstructure and residual stress improvement in wire and arc additively manufactured parts through high-pressure rolling[J]. *Journal of Materials Processing Technology*, 2013, 213(10):1782-1791.
- [14] Martina F, Colegrove P A, Williams S W, et al. Microstructure of Interpass Rolled Wire + Arc Additive Manufacturing Ti-6Al-4V Components[J]. *Metallurgical & Materials Transactions A*, 2015, 46(12):6103-6118.
- [15] Martina F, Roy M J, Szost B A, et al. Residual stress of as-deposited and rolled wire+arc additive manufacturing Ti-6Al-4V components[J]. *Materials Science & Technology*, 2016, 01:1-10.
- [16] Donoghue J, Antonysamy A A, Martina F, et al. The effectiveness of combining rolling deformation with wire-arc additive manufacture on  $\beta$ -Grain refinement and texture modification in Ti-6Al-4V[J]. *Materials Characterization*, 2016, 114:103-114.
- [17] Zhang H, Wang X, Wang G, et al. Hybrid direct manufacturing method of metallic parts using deposition and micro continuous rolling[J]. *Rapid Prototyping Journal*, 2013, 19(6):387-394.
- [18] Feng W, Fu Y. High temperature deformation behavior and constitutive modeling for 20CrMnTiH steel[J]. *Materials & Design*, 2014, 57(5):465-471.